Dissociation of excitons in Cu_2O by an electric field

J. Heckötter,[1] M. Freitag,[1] D. Fröhlich,[1] M. Aßmann,[1] M. Bayer,[1,2] M. A. Semina,[2] and M. M. Glazov[2]
[1]*Experimentelle Physik 2, Technische Universität Dortmund, D-44221 Dortmund, Germany*
[2]*Ioffe Institute, Russian Academy of Sciences, 194021, St.-Petersburg, Russia*

(Received 11 January 2018; revised manuscript received 21 May 2018; published 31 July 2018)

The electric field-induced dissociation is studied for excited states of the yellow exciton series of Cu_2O. With increasing principal quantum number n, corresponding to rising exciton energy, the field strength for dissociation decreases as expected. Surprisingly, within a manifold belonging to a particular n this trend is reversed as the required dissociation field increases with rising energy. In agreement with calculations we attribute this finding to the distribution of the exciton wave functions in the potential landscape. While the low energy states in the multiplet are shifted towards the side where the potential is lowered by the electric field, thereby facilitating dissociation, the high energy states are moved to the other side stabilizing them up to higher fields.

DOI: 10.1103/PhysRevB.98.035150

I. INTRODUCTION

Excitons in semiconductors are often considered to be the analogues of hydrogenlike atoms. Recent high-resolution studies of excitons in an external electric or magnetic field, also in the Rydberg regime, have revealed remarkable similarities but also striking differences to Rydberg atoms [1–5]. In case of a resemblance, its origin may still be distinctly different from atoms, as the exciton behavior is determined by solid state related features, in particular the energy bands dispersions. Even if the underlying physics is identical, for example, when the interaction with an external field becomes the dominant factor, excitons are worth to be examined in detail as they provide a unique platform for comprehensive bench-top studies of quantum effects which are considerably more difficult to access experimentally for atoms, in particular in the Rydberg regime [6]. This is due to the smaller exciton Rydberg energy, making excitons more susceptible to external fields. Fundamentally different from atoms is also the mixing of states with different angular momenta by the crystal environment, granting optical access to a large number of exciton states already in a single photon absorption.

Here we study the dissociation of excitons in Cu_2O subject to a homogeneous electric field. At weak fields, the field-induced tilt of the Coulomb potential describing the hydrogenlike exciton problem causes the evolution of Stark fans for each exciton multiplet. Oscillator strength is redistributed between the excitons resulting in rich optical spectra [3]. A further increase of the field leads to a vanishing potential barrier for the electron-hole relative motion so that exciton dissociation becomes possible. This is the regime that we focus on here. A preliminary result was obtained in Ref. [7] where we surprisingly observed for the principal quantum number $n = 11$ in the Rydberg series that states of high energy within the multiplet persist up to higher applied voltages compared to states of lower energy. From first sight one would expect the opposite, namely that states undergo dissociation the easier, the higher their energy is due to the lower tunneling barrier. This counterintuitive behavior was attributed to the centrifugal barrier in the radial part of electron-hole relative motion. A detailed analysis was, however, prevented by the large number of states in the $n = 11$ multiplet.

Here we study the exciton dissociation for n ranging from 3 to 10 which includes the onset of the Rydberg-excitons regime. The transition to the Rydberg regime has been roughly defined in our earlier work [1] to be at the $n = 6$ state, when the exciton size surpasses 100 nm and is about two orders of magnitude larger than in the ground state. We systematically confirm the previously observed trend and from the comprehensive set of data we develop a detailed understanding of the phenomenology: In a Stark fan with the given n, excitonic states that undergo energy shifts in applied electric field can be approximately described as dipoles oriented parallel or antiparallel to the field, which lowers or increases their energy. For high energy states the wave function is shifted to the opposite side of the dissociation barrier so that they are less prone to ionization, for low energy states the behavior is opposite. This qualitative picture is confirmed by calculations accounting for deviations from the hydrogenic model related with the crystal environment.

II. EXPERIMENTALS

The experiments were performed on bulklike cuprous oxide crystal slabs placed strain-free in a sample holder that allowed application of an electric field. The holder was placed at $T = 1.3$ K in the liquid helium insert of an optical cryostat. The electric field $\boldsymbol{F}$ was applied in longitudinal configuration along the optical axis chosen to be parallel to the [110] crystal axis, Fig. 1. The absorption was measured by a broadband white light source with the bandwidth reduced to the wavelength range of interest by a double monochromator. The light was polarized parallel to the $[1\bar{1}0]$ direction [8] (polarization vector $\boldsymbol{e}_1$ in Fig. 1). The excitation power was in the few μW range being, on one hand, high enough to obtain a good signal-to-noise ratio, but, on the other hand, low enough to avoid any notable line broadening and other many-body effects. After

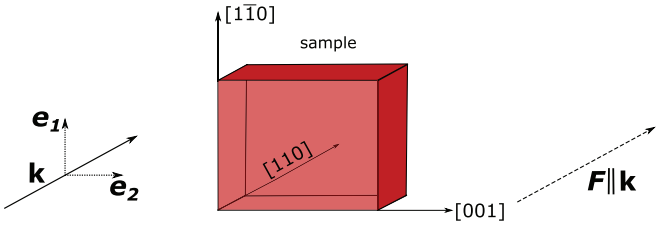

FIG. 1. Scheme of the experimental configuration. The light wave vector $\boldsymbol{k}$ is oriented along the [110] direction. The polarization of the light can be chosen to be parallel to the [1$\bar{1}$0] ($\boldsymbol{e}_1$) or the [001] ($\boldsymbol{e}_2$) direction (see Supplemental Material [9] for the latter case). The electric field $\boldsymbol{F}$ is applied along the optical axis.

transmission through the crystal, the light was dispersed by another double monochromator and detected by a Si-charge coupled device camera. The obtained spectral resolution of less than 10 μeV is sufficient for the states in question.

For completeness, we repeat some of the basic features of the yellow exciton series in cuprous oxide, elaborated previously in Refs. [1,2,18,19]: Due to the even parity of the topmost valence band and the lowest conduction band, electron-hole transitions are electric dipole forbidden. However, with account for the envelope wave function, excitons with P-type envelope (orbital angular momentum $l = 1$) become dipole allowed and dominate the absorption spectra. Across the whole exciton series, their energies for $n > 2$ follow to a good approximation the simple hydrogen formula $E_n = -Ry/n^2$ with the Rydberg energy $Ry = 86$ meV. Further, for their oscillator strength and the linewidth we find n^{-3} scaling laws for n up to 10, also in agreement with a hydrogenlike description. The linewidth is contributed by radiative decay and additionally by phonon scattering both following the same n^{-3} dependences on n. From the comparison with the theory, we also conclude that the lines up to $n = 10$ are mostly homogeneously broadened, so that we are not limited by the spectral resolution.

Taking a closer look, we find a splitting of each exciton line, so that the hydrogenlike angular momentum degeneracy is lifted. The splitting is caused by the symmetry reduction due to the crystal which affects mostly the valence band structure with strong deviations from a parabolic dispersion. As a consequence, states with different orbital angular momentum l become mixed, also resulting in the splitting [20]. Calculation of the exciton energies including the band structure details are complicated, in particular when adding external perturbations. As was demonstrated in Refs. [21,22], these details can be to a good approximation captured using the quantum defect concept, by which the exciton energy formula is modified to $E_{n,l} = -Ry/(n - \delta_{n,l})^2$ with the quantum defects $\delta_{n,l}$, so that the exciton energies depend both on n and l. The $\delta_{n,l}$ values, established from spectroscopy or theory, allow one to simplify calculations, for example in external fields, by comprising band structure details in them. As such, the quantum defect can be also a useful concept for any other class of semiconductors, provided that the exciton level spectrum can be resolved with similar precision as done here.

The size of the splitting of an exciton multiplet n is small compared to the splitting between states with different n. Moreover, the mixing of states with different l, which also causes a redistribution of the oscillator strength, is not too strong, thus in the following we still use the l notations to label them. The splitting within a multiplet decreases like n^{-3} so that for $n > 10$ the levels are quasidegenerate [7]. Qualitatively, this can be considered as a 'motional narrowing,' in which with increasing n the wave function extension becomes so large that the exciton is practically no longer affected by the symmetry reduction from the spherical symmetry of hydrogen to the cubic symmetry of Cu_2O.

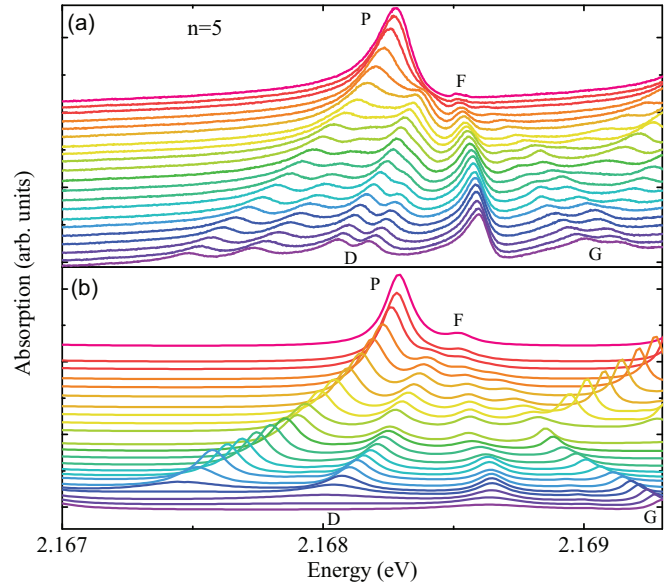

FIG. 2. (a) Absorption spectra of the $n = 5$ exciton for different voltages increasing from $U = 0$ (top trace) to 20 V in steps of 1 V. $\boldsymbol{F} \parallel [110]$, $\boldsymbol{e}_1 \parallel [1\bar{1}0]$. (b) Calculated absorption spectra, see text and Supplemental Material [9] for details.

III. EXPERIMENTAL RESULTS

Figure 2(a) shows the evolution of the exciton multiplet $n = 5$ in electric field. For $n = 5$, the exciton angular momentum $l \leq 4$, restricting the series to the G exciton. Hereafter we use the spectroscopic notation S, P, D, F, G, … to denote the $l = 0, 1, 2, 3, 4, \ldots$ hydrogenic states. In an electric field these states become mixed leading to complex superpositions [3]. For simplicity, we label, however, the states according to those from which they emerge at zero field. The zero field spectrum in Fig. 2(a) is dominated by the P exciton with a weak feature related to the F excitons on the high energy side, which are optically activated due to state mixing by the valence band structure [2,23]. The asymmetric lineshape, as most prominently seen for the P exciton, arises from interference effects with the background of phonon-assisted absorption by the $1S$ yellow excitons [24–26].

With increasing field the P exciton continuously shifts to lower energies and becomes weaker. On the other hand, the F exciton intensity steadily rises with some trend of saturation at high field. Additional features, particularly, the D excitons in between the P and F states emerge, mainly due to mixing with the P state, from which they obtain oscillator strength. They first become stronger and then start to fade away: This occurs at

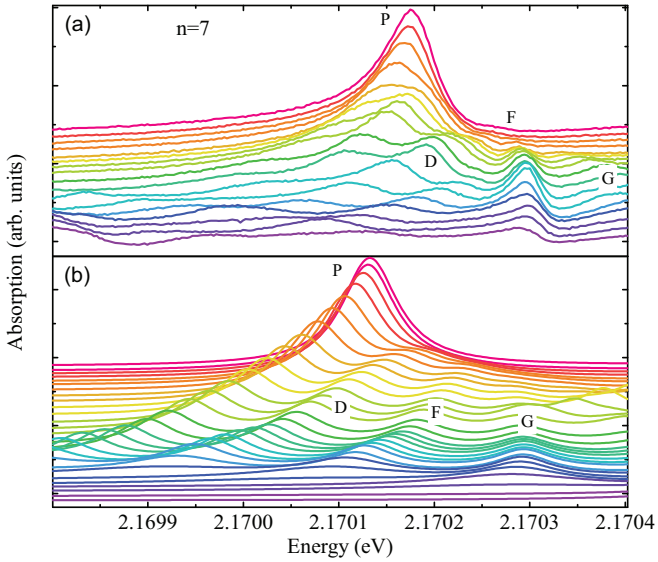

FIG. 3. (a) Absorption spectra of the $n = 7$ exciton for different voltages increasing from $U = 0$ (top trace) to 2 V in steps of 0.2 V and then to 9 V in steps of 1 V. $\boldsymbol{F} \parallel [110]$, $\boldsymbol{e}_1 \parallel [1\bar{1}0]$. (b) Calculated absorption spectra, see text and Supplemental Material [9] for details.

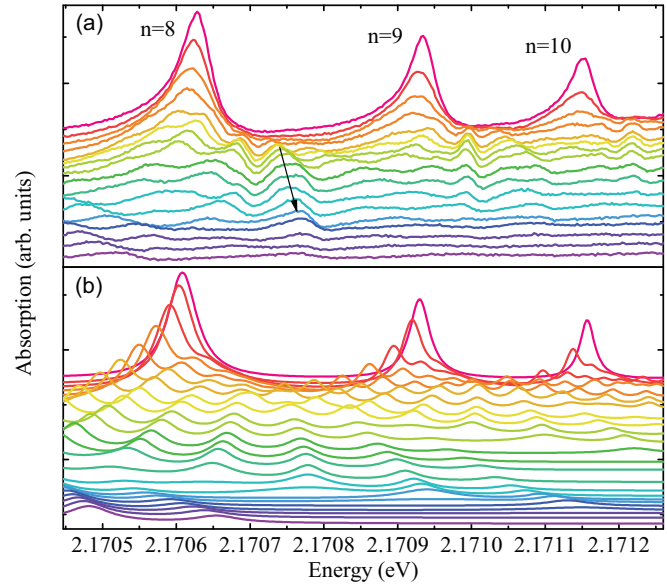

FIG. 4. (a) Absorption spectra in the energy range of the $n = 8$, 9, and 10 excitons for different voltages increasing from $U = 0$ (top trace) to 2 V in steps of 0.2 V and then to 9 V in steps of 1 V for the two lowest traces, respectively. $\boldsymbol{F} \parallel [110]$, $\boldsymbol{e}_1 \parallel [1\bar{1}0]$. The arrow indicates a complex absorption feature consisting of several states also from different n. (b) Calculated absorption spectra within the simplified model neglecting spin, spin-orbit, and exchange interactions, see text and Supplemental Material [9] for details.

larger voltages than for P, but at lower voltages than for F. On the high energy side, high angular momentum excitons appear which have to be associated with G excitons. They show a strong high energy shift and become continuously stronger up to the highest applied fields.

Figure 2(a) already clearly shows the main experimental result of our work: The states with higher transition energy within a multiplet are more robust with respect to field-induced dissociation than the lower energy states. This picture is corroborated for other exciton multiplets, for which we choose as an example $n = 7$, see Fig. 3(a). In general, the features vanish at much lower voltages than in the previous case, the applied voltages do not even reach half the values than used before to induce similar effects. This underlines that the ionization of higher-n states occurs at lower voltages. On the other hand, states on the high energy side of $n = 7$ gain oscillator strength by application of the field and remain visible even though the low energy states have already almost vanished due to ionization.

Increased complexity due to overlap of state multiplets is also evidenced in Fig. 4(a), showing the exciton spectra corresponding to $n = 8, 9$, and 10. The applied voltage range is restricted to 9 V in this case. From this overview the observed features can be comprehended: With increasing voltage the multiplets disappear, starting from the high energy side, while within a multiplet the trend is reversed, as most prominently seen for $n = 8$. However, clear distinction and precise assignment of the states become increasingly complicated, also because of the interpenetration of states from different n. Further, the density of states increases with n due to the larger allowed $l \leq n - 1$, and the states become closely spaced. In a simplified way, one may attribute the high energy lines as emerging solely from the F- or other high angular momentum excitons. However, care needs to be exercised here: Due to finite linewidth and crystal-induced state mixing, an absorption feature might be contributed by several states. This becomes obvious, e.g., for the absorption around 2.17075 eV, marked by the arrow in Fig. 4(a). The center of gravity of this absorption band shifts to higher energies. The sequence of states in the band vanishing from the low to the high energy flank with increasing voltage results in the observed net energy shift of this absorption feature.

IV. MODEL

To obtain a deeper understanding of the results, we consider first the case of a hydrogenlike system, neglecting the details of the semiconductor band structure. The deviations of the valence band from parabolic dispersion will be introduced below using the quantum defect concept [3,7,21]. The hydrogenic Hamiltonian for the relative motion of electron and hole in electric field $\boldsymbol{F}$ pointing along the z axis is given by

$$\mathcal{H}_0 = \frac{\boldsymbol{p}^2}{2\mu} - \frac{e^2}{\varepsilon r} - eFz, \tag{1}$$

which describes the relative motion of an effective negatively charged particle in a potential comprised of the Coulomb potential from a positive charge and the electrostatic energy of interaction with the electric field. Here $\boldsymbol{r} = (x, y, z)$ is the relative coordinate of electron and hole, $\boldsymbol{p} = -\mathrm{i}\hbar\partial/\partial\boldsymbol{r}$ is the relative motion momentum, μ is the reduced mass of electron and hole, e is the electron charge and ε is the dielectric constant of cuprous oxide. The electron effective mass is about the free electron mass m_0 in this material, while that of the valence band hole is about $0.6m_0$ [27].

To illustrate the field effect we use the basis states in the form $\Psi_{nlm}(\boldsymbol{r}) = R_{nl}(r)Y_{lm}(\vartheta, \varphi)$, where ϑ and φ are the angles

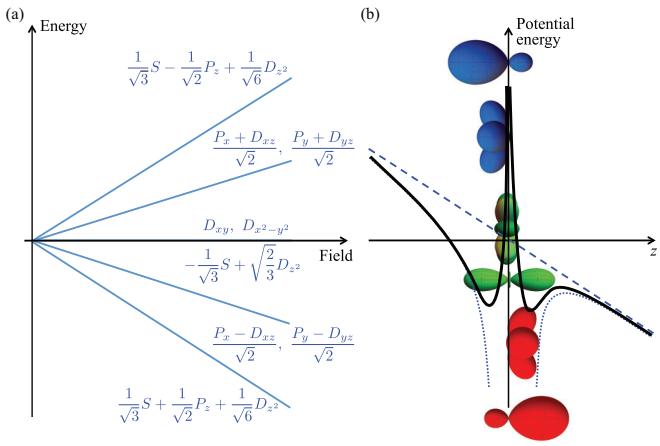

FIG. 5. (a) Scheme of the Stark fan for the multiplet with $n = 3$. The levels are marked by the zero-order eigenfunctions in electric field. (b) Schematic illustration of the eigenfunctions and the potential in electric field. The low (high) energy states, plotted with red (blue) color, have higher electron density at $z > 0$ ($z < 0$), i.e., closer to (farther from) the tunneling barrier. On the other hand, the states which do not obtain a dipole moment by state mixing in electric field (shown by the green contours), are still symmetric with respect to the field axis and do not show an energy shift.

of the position vector $\boldsymbol{r}$ in the spherical coordinate system with the polar axis z, $Y_{lm}(\vartheta, \varphi)$ are the angular harmonics, and $R_{nl}(r)$ are the radial functions. The effective potential for the radial motion contains, in addition to the Coulomb term, the centrifugal barrier $V_c(r) = \hbar^2 l(l+1)/(2\mu r^2)$, which is acting only on states with finite angular momentum $l \neq 0$, keeping the wave function away from the origin of the relative motion.

In the spherical approximation, according to the selection rules, only the excitons with P-type envelope can be excited in single photon absorption without electric field. When the field is applied ($\boldsymbol{F} \neq 0$), the symmetry is reduced leading to mixing of states with different angular momenta [3,28,29]. However, the rotational symmetry around the field is maintained so that the angular momentum component m along the z direction is conserved and only states with the same m become mixed. The new eigenstates are linear combinations of the zero field states and can demonstrate a dipole moment that is absent without field application. If present, this dipole moment becomes oriented by the electric field, leading to Stark energy shifts, as schematically illustrated in Fig. 5. The hydrogenic states $\Psi_{nlm}(\boldsymbol{r})$ are characterized by the parity $(-1)^l$, so that the charge distribution $|\Psi_{nlm}(\boldsymbol{r})|^2$ is symmetric, independent of l. In electric field, states of opposite parity are mixed, which leads to an amplification (reduction) of the wave function on one side of the centrifugal barrier and reduction (amplification) on the other side. This causes an asymmetry of the charge distribution along z, see Fig. 5. Within a Stark fan belonging to a particular n, for each state moving to higher energies there is a parity-conjugate state that is moving to lower energies. The same hydrogen wave functions contribute to a conjugate state but the relative phase between the states of opposite parity is inverted, so that also the dipole moment is inverted. As a result, the higher energy states whose dipole moment is aligned opposite to the field have higher probability density away from the tunnel barrier (shifted to the left in Fig. 5) while the lower energy states are shifted to the right, that is, towards the tunnel barrier at $z > 0$. The latter states can preferentially undergo tunneling and, hence, dissociate, despite their lower absolute energy and higher binding energy. This has to be contrasted with its conjugate state at higher energy, for which the probability distribution is inverted relative to the centrifugal barrier, making tunneling less probable, so that higher electric fields have to be applied in order to induce dissociation [30].

These qualitative arguments are supported by a quantitative analysis. We use parabolic coordinates to separate the variables in the Hamiltonian (1) and calculate the complex eigenenergies of the hydrogenic series [31–35]. Further, we construct an "effective Hamiltonian" which accounts for quantum defects and complex energies of the excitonic resonances [30,36], see Ref. [9] for details. The diagonalization of this effective Hamiltonian $\mathcal{H}$ provides the eigenstates Ψ_k and the complex energies $\mathcal{E}_k = E_k - \mathrm{i}\Gamma_k$, where k enumerates the eigenstates, which are then used to calculate the transmission spectra in the framework of the approach developed in Ref. [3]. The optical density of the cuprous oxide film calculated in that way for the energy range of the $n = 3 \ldots 6$ excitons is shown in Fig. 6 for the light propagation direction $\boldsymbol{k} \parallel [110]$ and the light polarization vector $\boldsymbol{e}_1 \parallel [1\bar{1}0]$. The voltage was converted in an electric field using the coefficient determined in Ref. [3]. Figure 6 clearly shows the fine structure of the exciton states, including that of the P excitons, and the emergence of higher angular momentum states, e.g., of the F states for $n \geq 4$. It also demonstrates the dissociation of excitons: In agreement with the analysis above, (i) the multiplets with higher n dissociate at smaller fields as compared to those with smaller n, while (ii) the states with higher energy in the multiplet dissociate at larger fields. The overall agreement of the calculated spectra with the measured ones is good.

A detailed comparison of theory with experiment as a function of electric field is provided in the lower panels (b) of Figs. 2 to 4. For the $n = 5$ multiplet in Fig. 2(b), the calculations take into account also the contributions of lower and higher n states and accurately reproduce the line shifts in the range of small fields. There are slight differences between the observed and calculated line positions and intensities. We emphasize that we did not target fully quantitative agreement between theory and experiment, but rather used the same set of established material parameters for describing the field dispersions of all multiplets. Note that the studied energy ranges are quite small, in case of $n = 5$ only 2 meV and in case of $n = 7$ even only 0.5 meV, for example. Moreover, the observed lines have significantly larger spectral widths than in theory, which we attribute to the additional relaxation mechanisms by phonon scattering or radiative decay that are not considered in the calculations. As a consequence, some lines and their evolution cannot be as clearly resolved, but still the main trends can be assessed.

Importantly, extra lines appear in the experimental data. From their identical shifts with increasing electric field we conclude that the P exciton appears to be split into a doublet, and the same holds for the D exciton, while in theory both are given by a single line. These differences may be attributed to deviations from the ideal situation, possibly, due to a slight deviation of the field orientation from the nominal [110] crystallographic axis, formation of domains in the crystal

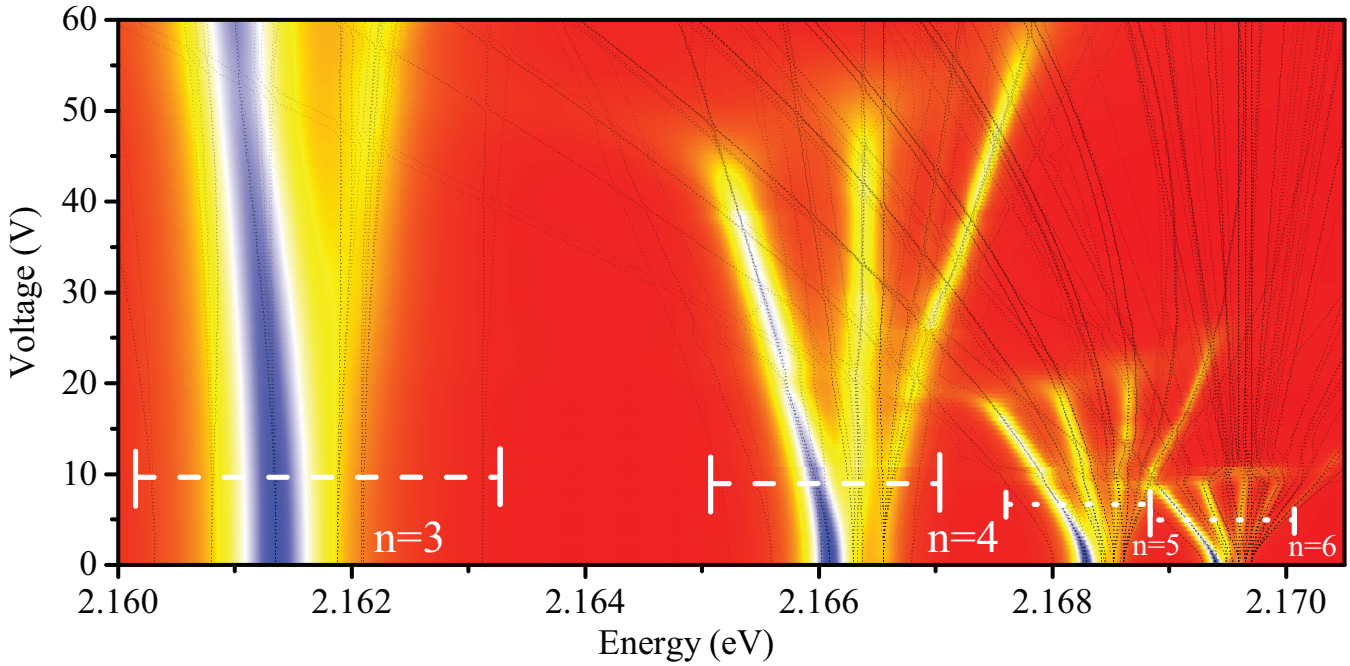

FIG. 6. Optical density (false color scale) of the Cu_2O slab calculated within the developed model in the energy range of the $n = 3 \ldots 6$ excitons. $\boldsymbol{F} \parallel [110]$, $\boldsymbol{e}_1 \parallel [1\bar{1}0]$.

with slightly different orientations, presence of uncompensated charges at surfaces or defects etc. [3]. The splitting of the $P-$ and the $D-$ levels most likely also explains the observation of a dominance of the F excitons at high applied voltage compared to the S and D excitons. Here further studies are necessary, also with respect to the potential of preparing crystals with even higher purity. Otherwise the experimental features are well reproduced, in particular with regard to the variation of the dissociation with the state energy.

The agreement is similarly good for $n = 7$ and $n = 8, 9, 10$ in Figs. 3 and 4. Note that the calculations for $n = 8 \ldots 10$ were done within a simplified model where the spin degrees of freedom of electron and hole are disregarded and, correspondingly, the spin-orbit and exchange interaction are neglected. Thereby the spectra can be calculated within a reasonable computation time. Despite the simplicity of the model, the overall behavior of the spectra is still close to that in experiment, as in the case for $n = 7$. The enhanced stability of states on the high energy side of a multiplet with particular principal quantum number is in good agreement with experiment. Simultaneously smaller voltages need to be applied for inducing exciton dissociation when states belonging to higher n are considered.

V. CONCLUSION

We have performed detailed studies of the dissociation of yellow excitons in cuprous oxide by an electric field which have demonstrated that not only the energy, but also the wave function of a state is important for understanding its dissociation. This dependence may be exploited, for example, to isolate a particular exciton state and study collective effects between these dipolar excitons such as a possible condensation.

ACKNOWLEDGMENTS

We acknowledge the support of this project by DFG and the RFBR in the frame of TRR 160 (projects A1 and 15-52-12012) and by the DFG in the DFG SPP 1929 GiRyd and Grant No. AS 459/1-3. M.M.G. was partially supported by RF President Grant No. MD-1555.2017.2. M.B. acknowledges support by RF Government Grant No. 14.Z50.31.0021. M.A.S. acknowledges support by the program of Presidium of RAS "Nanostructures: Physics, Chemistry, Biology, Fundamentals of technology."

[1] T. Kazimierczuk, D. Fröhlich, S. Scheel, H. Stolz, and M. Bayer, Giant rydberg excitons in the copper oxide Cu_2O, Nature (London) **514**, 343 (2014).

[2] J. Thewes, J. Heckötter, T. Kazimierczuk, M. Aßmann, D. Fröhlich, M. Bayer, M. A. Semina, and M. M. Glazov, Observation of High Angular Momentum Excitons in Cuprous Oxide, Phys. Rev. Lett. **115**, 027402 (2015).

[3] J. Heckötter, M. Freitag, D. Fröhlich, M. Aßmann, M. Bayer, M. A. Semina, and M. M. Glazov, High-resolution study of the yellow excitons in Cu_2O subject to an electric field, Phys. Rev. B **95**, 035210 (2017).

[4] F. Schweiner, J. Main, G. Wunner, M. Freitag, J. Heckötter, C. Uihlein, M. Aßmann, D. Fröhlich, and M. Bayer, Magnetoexcitons in cuprous oxide, Phys. Rev. B **95**, 035202 (2017).

[5] M. Aßmann, J. Thewes, D. Fröhlich, and M. Bayer, Quantum chaos and breaking of all anti-unitary symmetries in Rydberg excitons, Nat. Mater. **15**, 741 (2016).

[6] P. Grünwald, M. Aßmann, J. Heckötter, D. Fröhlich, M. Bayer, H. Stolz, and S. Scheel, Signatures of Quantum Coherences in Rydberg Excitons, Phys. Rev. Lett. **117**, 133003 (2016).

[7] J. Heckötter, M. Freitag, D. Fröhlich, M. Aßmann, M. Bayer, M. A. Semina, and M. M. Glazov, Scaling laws of Rydberg excitons, Phys. Rev. B **96**, 125142 (2017).

[8] In this configuration the quadrupole allowed transitions to the S and D excitons are absent at $F = 0$ [3], and such geometry is chosen to simplify the appearance of the spectra and enable identification of the absorption lines. For developing a complete picture, we also recorded spectra for [001] polarization which are presented in the Supplemental Materials [9].

[9] See Supplemental Material at http://link.aps.org/supplemental/10.1103/PhysRevB.98.035150, that include Refs. [10–17], for details on theoretical calculations and additional experimental data.

[10] R. J. Damburg and V. V. Kolosov, A hydrogen atom in a uniform electric field, J. Phys. B **9**, 3149 (1976).

[11] V. M. Vainberg, V. D. Mur, V. S. Popov, and A. V. Sergeev, The hydrogen atom in a strong electric field, J. Exp. Theor. Phys. **66**, 258 (1987).

[12] V. D. Mur and V. S. Popov, Stark effect exhibited by Rydberg atoms and the near-threshold resonances of the photoionization cross section, J. Exp. Theor. Phys. **67**, 2027 (1988).

[13] V. D. Mur, V. S. Popov, A. V. Sergeev, and A. V. Shcheblykin, Stark resonances and scaling in Rydberg atoms, J. Exp. Theor. Phys. **69**, 49 (1989).

[14] V. S. Popov, V. D. Mur, and A. V. Sergeev, Theory of the Stark effect in a strong field: Critical fields, above-barrier resonances, dependence on dimensionality, J. Exp. Theor. Phys. **79**, 547 (1994).

[15] W. E. Cooke and T. F. Gallagher, Dependence of Rydberg-state field-ionization thresholds on $|m_l|$, Phys. Rev. A **17**, 1226 (1978).

[16] David Park, Relation between the parabolic and spherical eigenfunctions of hydrogen, Z. Phys. **159**, 155 (1960).

[17] A. R. Edmonds, *Angular Momentum in Quantum Mechanics* (Princeton University Press, Princeton, NJ, 1974).

[18] R. J. Elliott, Intensity of optical absorption by excitons, Phys. Rev. **108**, 1384 (1957).

[19] V. T. Agekyan, Spectroscopic properties of semiconductor crystals with direct forbidden energy gap, Phys. Status Solidi A **43**, 11 (1977).

[20] Strictly speaking, the degeneracy in the magnetic quantum number as well as in the spin indices of electron and hole is also lifted due to the reduced symmetry and the spin-orbit and exchange interactions. These effects are unimportant for the following discussion.

[21] F. Schöne, S.-O. Krüger, P. Grünwald, H. Stolz, S. Scheel, M. Aßmann, J. Heckötter, J. Thewes, D. Fröhlich, and M. Bayer, Deviations of the exciton level spectrum in Cu_2O from the hydrogen series, Phys. Rev. B **93**, 075203 (2016).

[22] F. Schöne, S.-O. Krüger, P. Grünwald, M. Aßmann, J. Heckötter, J. Thewes, H. Stolz, D. Fröhlich, M. Bayer, and S. Scheel, Coupled valence band dispersions and the quantum defect of excitons in Cu_2O, J. Phys. B **49**, 134003 (2016).

[23] F. Schweiner, J. Main, M. Feldmaier, G. Wunner, and C. Uihlein, Impact of the valence band structure of Cu_2O on excitonic spectra, Phys. Rev. B **93**, 195203 (2016).

[24] Y. Toyozawa, Interband effect of lattice vibrations in the exciton absorption spectra, J. Phys. Chem. Solids **25**, 59 (1964).

[25] T. Ueno, On the contour of the absorption lines in Cu_2O, J. Phys. Soc. Jpn. **26**, 438 (1969).

[26] A. Jolk and C. F. Klingshirn, Linear and nonlinear excitonic absorption and photoluminescence spectra in Cu_2O: Line shape analysis and exciton drift, Phys. Status Solidi B **206**, 841 (1998).

[27] N. Naka, I. Akimoto, M. Shirai, and K.-I. Kan'no, Time-resolved cyclotron resonance in cuprous oxide, Phys. Rev. B **85**, 035209 (2012).

[28] V. T. Agekyan, B. S. Monozon, and I. P. Shiryapov, The fine structure of Wannier-Mott excitons in a cubic crystal and its behavior in an electric field, Phys. Status Solidi B **66**, 359 (1974).

[29] S. Zielińska-Raczyńska, D. Ziemkiewicz, and G. Czajkowski, Electro-optical properties of Rydberg excitons, Phys. Rev. B **94**, 045205 (2016).

[30] T. F. Gallagher, *Rydberg Atoms*, Cambridge Monographs on Atomic Physics (Cambridge University Press, Cambridge, 2005).

[31] L. D. Landau and E. M. Lifshitz, *Quantum Mechanics: Non-Relativistic Theory*, Vol. 3 (Butterworth-Heinemann, Oxford, 1977).

[32] I. A. Merkulov, Influence of exciton effect on electroabsorption in semiconductors, J. Exp. Theor. Phys. **39**, 1140 (1974).

[33] A. G. Aronov and A. S. Ioselevich, Effect of electric field on exciton absorption, J. Exp. Theor. Phys. **47**, 548 (1978).

[34] S. Yu. Slavyanov, *Asymptotic solutions of the one-dimensional Schrödinger equation*, Translations of mathematical monographs, Vol. 151 (American Mathematical Society, Providence, Rhode Island, 1996).

[35] I. P. Areshev, Two-photon excitonic light absorption in semiconductors in a static electric field, Sov. Phys. Solid State **21**, 447 (1979).

[36] M. G. Littman, M. L. Zimmerman, and D. Kleppner, Tunneling Rates for Excited States of Sodium in a Static Electric Field, Phys. Rev. Lett. **37**, 486 (1976).